Power Electronics and Drives
3(38), No. 1, 2018 DOI: 10.2478/pead-2018-0014

sciendo

Power Electronics and Drives

Model Predictive Control of Four-Leg Three-Level Flying Capacitor Converter: Influence of Model Parameter Mismatch

Research Article

Kamil Antoniewicz[1], Krzysztof Rafal[1], Marek Jasinski[2]

[1] *Warsaw University of Technology, Institute of Heat Engineering, Nowowiejska 21/25, Warsaw, Poland*
[2] *Warsaw University of Technology, Institute of Control and Industrial Electronics, Koszykowa 75, Warsaw Poland*

Received June 06, 2018; Accepted July 20, 2018

Abstract: This paper presents a control method for a four-leg three-level flying capacitor converter (FCC) operating as a shunt active power filter (SAPF), based on model predictive control with finite number of control states (FS-MPC). Current control and capacitor voltage balancing are described. Influence of the mismatch of the inductive filter model parameters on the current control precision is analysed. Results are supported by the experimental waveforms obtained with a 10kVA set-up.

Keywords: *Multilevel converter • Current control • Model predictive control (MPC) • Shunt active power filter (SAPF)*

1. Introduction

Non-linear loads connected to the power network are the source of many undesirable phenomena, e.g. additional power losses in the network or negative influence on the grid voltage waveform shape (Strzelecki and Supronowicz, 2000). A common solution for issues caused by these loads is installation of filters that compensate the high-frequency harmonics of currents. Some of the popular types that should be mentioned are shunt passive, active and hybrid filters (Akagi, 1996).

Passive filters are designed for specified frequencies on the basis of resonant circuits consisting of inductors and capacitors (LC). They create a low-impedance loop between the load and the filter for current harmonics. Therefore, high-frequency harmonics are not transmitted to the power network.

Active filters are designed at the basis of power electronic converters, usually voltage source converters (VSCs). With an appropriate control method, they are able to generate currents of specified shape, to compensate the distortions introduced by the load and obtain a sinusoidal shape of grid currents. Moreover, their operation allows the compensation of reactive power and current imbalance (Akagi, 2006).

In recent decades, many current control methods for VSCs have been developed. One of the most interesting categories here is predictive control (PC) (Orlowska-Kowalska et al., 2014; Falkowski and Sikorski, 2018; Antoniewicz and Rafal, 2017; Sobanski, 2017). It was presented about 50 years ago, designed for the chemical industry. The dynamic development of microprocessors made application of that method possible for power electronics, where a real-time operation is required (Grodzki et al., 2011). In general, predictive control is based on the model (MPC) of the considered device, which allows calculation of values of selected variables, depending on possible states of control signals.

* *Email: kamil.antoniewicz@itc.pw.edu.pl, krafal@itc.pw.edu.pl, mja@isep.pw.edu.pl*

Open Access. © 2018 Kamil Antoniewicz et al., published by Sciendo. BY-NC-ND This work is licensed under the Creative Commons Attribution NonCommercial-NoDerivatives 4.0 License.

2. Four-leg three-level flying capacitor converter operating as a shunt active filter

The three-phase four-leg flying capacitor converter (FCC) topology operating as a shunt active power filter (SAPF) is presented in Fig. 1. The converter is connected to the grid via an inductive passive filter L_g at the point of common coupling (PCC), in parallel to the non-linear load.

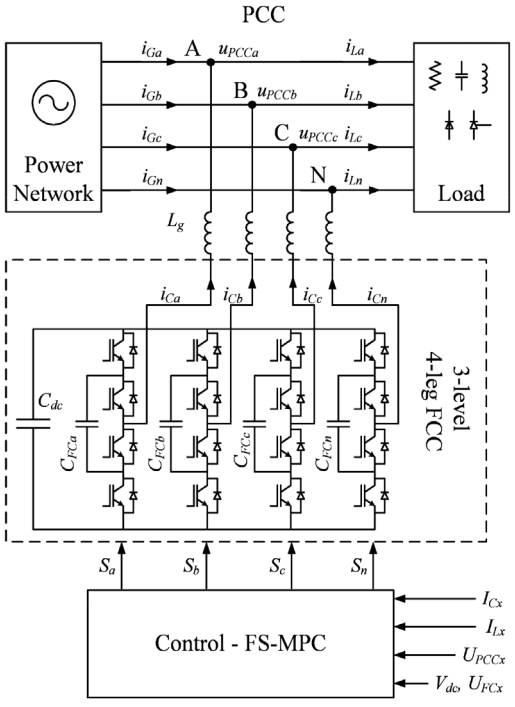

Fig. 1. A three-level four-leg FCC

In the FCC, each leg contains an additional flying capacitor C_{FC} and its voltage is equal to half of the C_{dc} capacitor direct current (DC) voltage. There are four allowed combinations of switching states in the leg. Two combinations cause that the output voltage of the leg relative to the negative busbar is 0 or V_{dc}. The other two states result in an output voltage of $½V_{dc}$. Each of these two redundant states can have one of two opposite effects on the C_{FC} capacitor voltage – charging or discharging. A choice of one of them is made on the basis of the output current direction and the voltage value on the respective capacitor in relation to the commanded value (in the three-level system V_{FC}=$½V_{dc}$). In the described method, voltage regulation is performed outside the main control loop; from the level of the prediction algorithm, only one of three output voltage levels is set (Antoniewicz and Jasinski, 2016b). Another solution is to include voltage balancing for the predictive control loop (Defay et al., 2008). Operation of the converter as an SAPF requires measurement of i_{Cx} converter currents and i_{Lx} load currents (where x index refers to phases a, b, c or neutral n wires). Distortions of the load currents i_{Lx} are compensated by the i_{Cx} filter current; thus, their level in the grid currents i_{Gx} is minimised. The relation can be formulated as follows:

$$i_{G,m}(t) = -i_{C,m}(t) + i_{L,m}(t) \tag{1}$$

Assuming the symmetry of voltages v_{PCC} at the PCC and the value of the neutral current of the grid $i_{Gn} = 0$, the above expression can be written as follows:

$$\begin{aligned} i_{L,n}(t) &= -\left(i_{La}(t)+i_{Lb}(t)+i_{Lc}(t)\right) \\ i_{C,n}(t) &= i_{L,n}(t) \\ i_{G,n}(t) &= 0 \end{aligned} \tag{2–4}$$

Equations (1)–(4) describe the currents and operation of a four-leg SAPF mathematically. Therefore, it shapes the output currents i_C of the converter to achieve three goals, namely, to compensate for higher harmonics, passive component of load currents i_L and their imbalance.

3. Finite states-set MPC

The regulation of higher harmonics of the current requires an algorithm ensuring very good dynamic behaviour. Traditional methods based on linear proportional-integral regulators may be too slow here. In order to increase their suitability for the regulation of higher harmonics, it is suggested to connect resonance modules in parallel. However, this solution still has an unsatisfactory step response.

Another possible control method is the use of hysteresis controllers. Despite the excellent dynamics, these are characterised by a variable switching frequency and the difficulties associated with filtering high-frequency components of the converter current. Comparison of the hysteresis control method with FS-MPC is presented by Antoniewicz and Jasinski (2016a). The following predictive control method allows elimination of disadvantages of the above solutions, providing good dynamics and stabilisation of switching frequencies. It also provides the ability to simultaneously control many variables by incorporating them into one common cost function (Rodriguez et al., 2013). The block diagram of the FS-MPC is shown in Fig. 2.

The fundamental block of this method is an object model that allows calculation of the value of its variables in the next steps of prediction. On the basis of the converter leg equation (with an appropriate voltage at the PCC), an expression was developed in which v_{PCCyx} (between the wires x and y) voltage was used (Antoniewicz and Jasinski, 2016b):

$$\begin{aligned} i_{pre,yx}(k+1) = &\frac{T_s}{R_g T_s + L_g}\left[V_{dc}\left(S_y - S_x\right) - \left(u_{PCCy}(k+1) - u_{PCCx}(k+1)\right)\right] \\ &+ \frac{L_g}{R_g T_s + L_g}\left[i_{Cy}(k) - i_{Cx}(k)\right] \end{aligned} \tag{5}$$

Assuming that $R_g = 0$, the equation can be simplified as follows:

$$\begin{aligned} i_{pre,yx}(k+1) = &\frac{T_s}{L_g}\left[V_{dc}\left(S_y(k+1) - S_x(k+1)\right) - \left(u_{PCCy}(k) - u_{PCCx}(k)\right)\right] \\ &+ \left[i_{Cy}(k) - i_{Cx}(k)\right] \end{aligned} \tag{6}$$

where T_s is the sampling period, k is the step index of the control algorithm; i_{pre} and i_C are the predicted and measured current values of the converter; L_g and R_g are the inductance and resistance of the grid filter; and the indices y and x refer to the converter's legs ($x \neq y$).

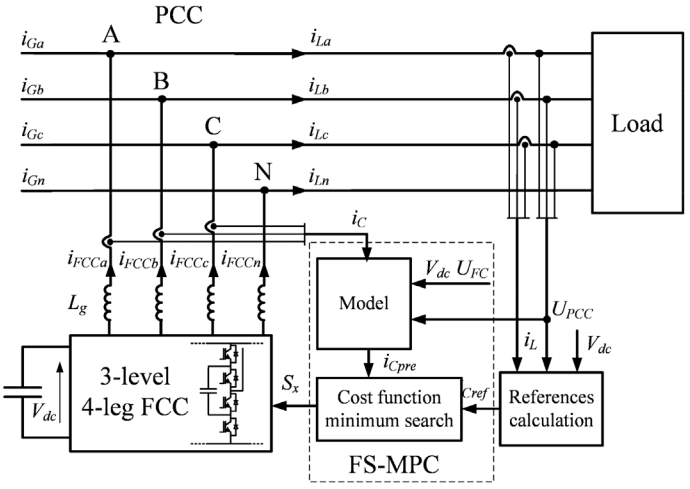

Fig. 2. Block diagram of predictive control

Operation of the converter as an SAPF requires the correct calculation of the reference current values of the converter satisfying the conditions represented by Eqs. (1)–(4). To calculate them, the instantaneous power theory is used (Akagi, 2007). The voltages and currents are transformed to a stationary coordinate reference frame, from which the instantaneous power values are calculated:

$$p_L = v_{PCC\alpha} i_{L\beta} + v_{PCC\beta} i_{L\alpha} \tag{7}$$

$$q_L = -v_{PCC\beta} i_{L\alpha} + v_{PCC\alpha} i_{L\beta} \tag{8}$$

The SAPF task is to eliminate the reactive power q_L and the active power variable component p_{Lvar} of the load. At the same time, a U_{dc} control loop sets the value of the active power p_{dc} necessary to cover losses in the converter. Finally, the converter reference power values are obtained as follows:

$$p_C = p_{Lvar} + p_{dc} \tag{9}$$

$$q_C = q_L \tag{10}$$

The reference current values i_{Cref} can therefore be calculated from the following equations:

$$\begin{bmatrix} i_{Cref\alpha} \\ i_{Cref\beta} \end{bmatrix} = \frac{1}{v_{PCC\alpha}{}^2 + v_{PCC\alpha}{}^2} \begin{bmatrix} v_{PCC\alpha} & -v_{PCC\beta} \\ v_{PCC\beta} & v_{PCC\alpha} \end{bmatrix} \begin{bmatrix} p_C \\ q_C \end{bmatrix} \tag{11}$$

and transformed into a natural coordinate reference frame.

The reference values are then compared with the i_{Cpre} values predicted from the model (5) or (6) and used to calculate the cost function J:

$$\begin{aligned} J\left(S_{abcn}(k+1)\right) = {} & w_{f1} \sum_{y=a,b,c} abs\left(i_{Cref,yn}(k+1) - i_{pre,yn}(k+1)\right) \\ & + w_{f2} \sum_{x,y=a,b,c,n} abs\left(i_{Cref,yx}(k+1) - i_{pre,yx}(k+1)\right) \end{aligned} \tag{12}$$

where w_{f1} is the weighting factor for the error of the phase currents and w_{f2} is the weighting factor for the error of the line currents.

The predicted values are calculated based on the measurements of the SAPF currents, the voltage at the PCC and the DC-link voltage for the finite set of future states of the switches $S(k + 1)$. In addition, it is necessary

to compensate for delays in the real system caused by the control platform, which is at least one sampling period. This function can be performed based on Eq. (5) or (6) for prediction, as described for instance in Antoniewicz and Jasinski (2016b).

The number of possible switching states for the proposed converter is $4^4 = 256$. Assuming that two of the four states in each leg are redundant, their total number is limited to $3^4 = 81$. For these states, the cost function indicator is calculated. Its minimum value determines the state of the switches, which is chosen in the next sampling period. Implementation of the independent voltage control loop for FCs allows reduction of the number of states necessary for analysis and significantly reduces the calculation time of the FS-MPC algorithm.

An important feature of the FS-MPC method is the dependence of its accuracy on matching the parameters of the model to the actual system (Rodriguez et al., 2013). In the paper, the expression (5) was used in the control, where the L_g inductance of the grid filter, besides measuring errors, has the greatest influence on the accuracy of the current prediction. In practice, the inductance of the grid choke may differ from the nominal one (typical tolerance of the values is $\pm 20\%$) and may vary depending on the frequency and instantaneous value of the current. To examine this phenomenon, an analysis of the influence of inductance mismatch on the algorithm's work was made. As an additional variable for analysis, the resistance of the grid filter was assumed, which was neglected to simplify prediction equations.

It should also be noted that choosing the value of weight coefficients (w_{f1} and w_{f2}), which are responsible for the influence of a given variable or error on the selection of switching state, has an impact on the SAPF operation. In order to analyse these relations, tests were performed with varying values of the selected factor. The results are presented in the further part of the paper.

4. Experimental results

The described control method has been implemented in the laboratory set-up. The basic parameters are summarised in Table 1. The control unit used in the experiment is the dSPACE1006mp platform. During the tests, a non-linear, asymmetrical load model was used, the scheme of which is shown in Fig. 3 (both loads were connected in parallel). The results were recorded using the Tektronix DPO5104B and TDS5034B digital oscilloscopes and then analysed with MatLab.

Table 1. Parameters of the laboratory set-up

Parameter	Value
Converter rated power	10 kVA
Grid voltage	3 × 400 V
DC-link voltage	700 V
DC-link capacitor capacitance	1.5 mF
Flying capacitor capacitance	250 μF
Grid filter inductance	1.5 mH
Sampling frequency	30 kHz

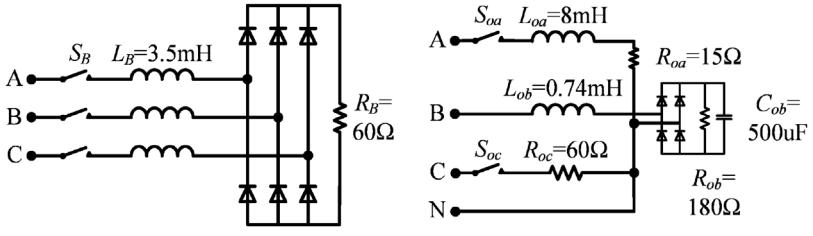

Fig. 3. Non-linear load model

The operation of the SAPF controlled by the FS-MPC method is shown in Fig. 4. On the waveforms, the red lines indicate the moment of switching on the phases A and C of the unbalanced load (first line) and the three-phase diode bridge (the second line). An experimental verification was carried out to determine the effect of mismatch of model parameters on the operation of the FS-MPC algorithm. Since the main purpose of the control is to maintain

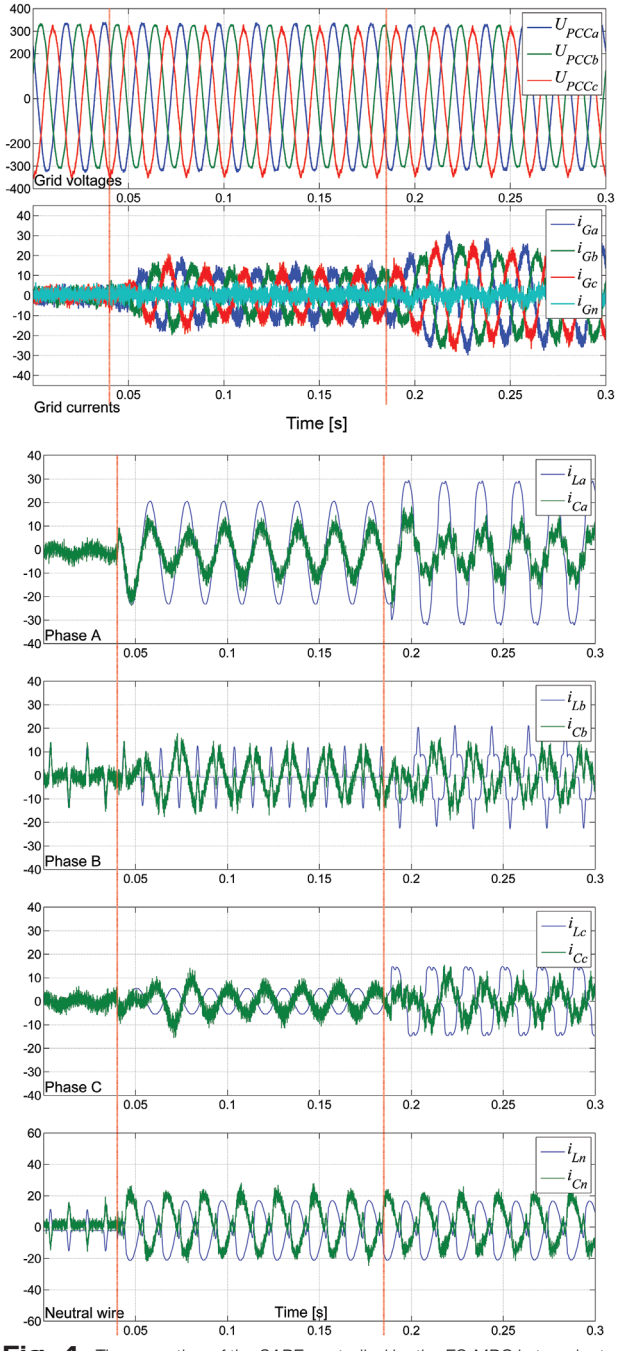

Fig. 4. The operation of the SAPF controlled by the FS-MPC in transient states (red lines) and steady state. From the top: grid voltages and currents, i_{Lx} load and i_{Cx} compensating currents

the sinusoidal grid current, the total harmonic distortion (THD) coefficient of the grid current THD(i_G), calculated to the 50th harmonic, has been selected as a quantitative indicator. As parameters, inductance and resistance of the grid filter introduced into the model were assumed. The results are illustrated in Fig. 5, independently for each phase. It can be noticed that underestimating the inductance of the filter by $>30\%$ causes a drastic increase in the THD(i_G). On the other hand, overestimation of this parameter even by $>50\%$ does not cause significant distortion. It can be noticed that the introduction of the resistance parameter into the model does not significantly affect the algorithm's operation. Omitting the filter resistance in Eq. (6) to simplify the calculations is therefore fully justified.

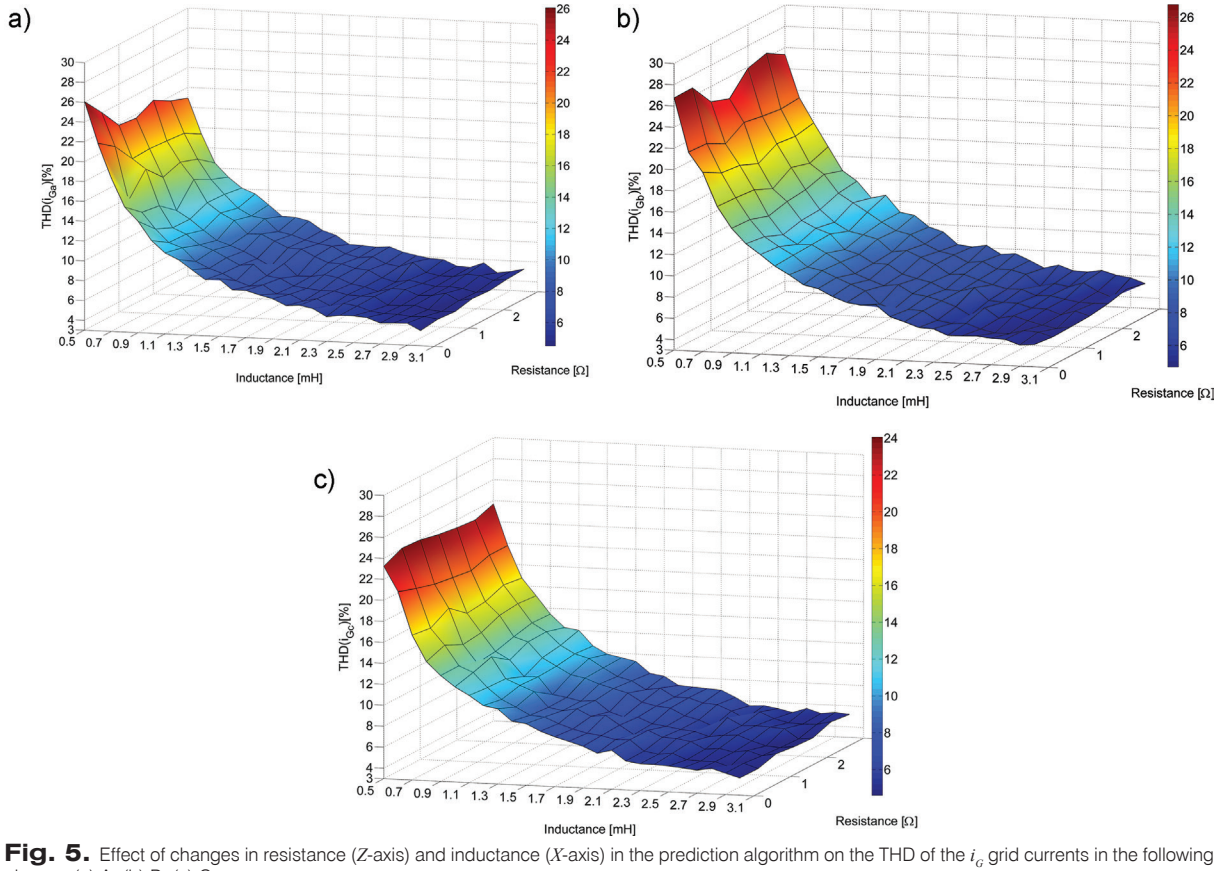

Fig. 5. Effect of changes in resistance (*Z*-axis) and inductance (*X*-axis) in the prediction algorithm on the THD of the i_G grid currents in the following phases: (a) A; (b) B; (c) C

In the next series of experiments, the influence of the weight coefficients proposed for calculating the cost function was examined. Coefficient w_{f1} is the weight of the phase current error and the coefficient w_{f2} is the line current. By default, both coefficients assume a value of one. The results are summarised in Fig. 6. In the case of increase in the coefficient w_{f1}, there is a tendency for a slow increase in the THD(i_G) coefficient of currents in all phases of the grid. This means a negative effect of the increase in the value of the weight coefficient of the phase current error in relation to the weight coefficient of the line currents. In addition, for the value of 0.1, it was possible to adjust the current in the neutral wire and ensure stable operation of the entire system.

In the case of a change in the coefficient w_{f2}, taking too low a value leads to an increase in the THD(i_G) coefficient in all phases. The operation of the algorithm improves when the coefficient in w_{f2} is increased, to stabilise after reaching the value of one. Further increase in its value has no significant effect on the algorithm's work.

5. Summary

The paper discusses the use of MPC with finite number of control states (FS-MPC) for a four-leg three-level FCC operating as an SAPF. Experimental results showing the effect of the mismatch of model parameters and cost function weighting factors on the algorithm's efficiency were presented, measured by the THD of the grid current.

Based on the presented implementation of the control algorithm and the experimental results, the following conclusions can be drawn:

- The model based on the description of line voltages and current quantities allows simplification of the model and limiting the amount of calculations;
- The FS-MPC algorithm ensures the high dynamics necessary to control the current of the SAPF;

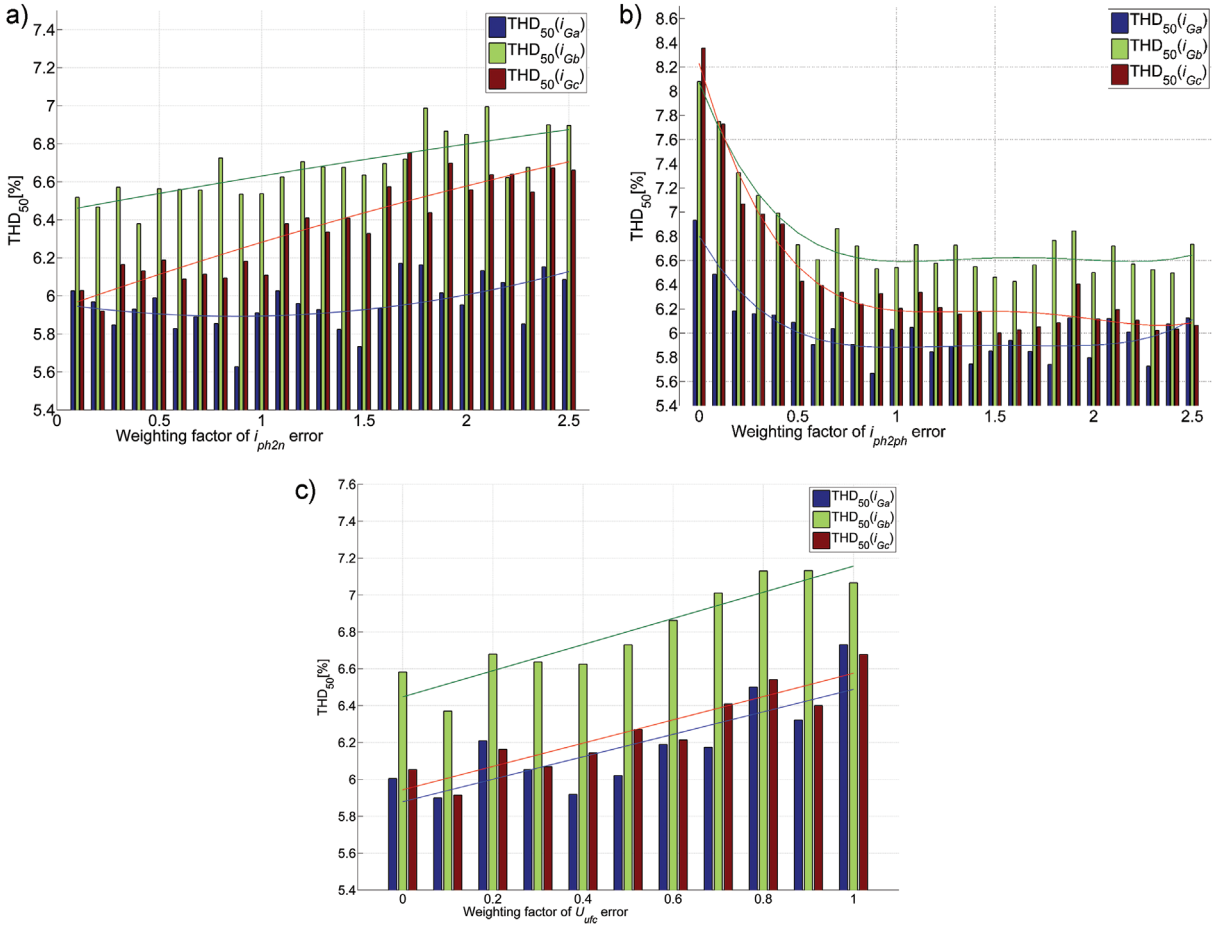

Fig. 6. The effect of change in the weight coefficients on the THD coefficient of the grid currents with regard to (a) w_{f1} (phase currents), (b) w_{f2} (line currents) and (c) wf_{Ufc} (FC voltage errors)

- Selection of a lower inductance value in the model than the actual one causes a drastic increase in the THD of the grid current. Overestimation of inductance does not significantly affect operation of the control algorithm;
- The filter resistance variations in the model do not significantly affect effectiveness of the control. The resistance can thus be omitted to simplify calculations;
- In the proposed cost function, the weighting factor w_{f1} assigned to the phase currents must be >0, because, unlike w_{f2}, it also refers to the current in the neutral wire. However, further increase of w_{f1} does not lead to a significant improvement of the system operation;
- A significant influence on the grid current THD(i_G) value is caused by w_{f2}, responsible for the line currents; $w_{f2} > w_{f1}$ results in an improvement in THD factors.

The proposed control method can be optimised for implementation on an industrial microcontroller. It can be concluded that it is an attractive solution for SAPF used in the industry.

Acknowledgement

The project was partially financed by the National Science Centre through grant number DEC-2013/09/B/ST7/01608.

References

Akagi, H. (1996). New Trends in Active Filters for Power Conditioning. *IEEE Transactions on Industry Applications*, 32(6), pp. 1312–1322.

Akagi, H. (2006). Modern Active Filters and Traditional Passive Filters. *Bulletin of the Polish Academy of Sciences. Technical Sciences*, 54, pp. 255–269.

Akagi, H., Watanabe, E. H. and Aredes, M. (2007). *Instantaneous Power Theory and Applications to Power Conditioning*. USA: IEEE Press-Wiley (IEEE Press Series on Power Engineering). [ISBN: 978-0-470-10761-4]

Antoniewicz, K. and Jasinski, M. (2016a). Experimental comparison of hysteresis based control and finite control state set Model Predictive Control of Shunt Active Power Filter," In: *2015 Selected Problems of Electrical Engineering and Electronics (WZEE),* Kielce, Poland, 17–19 September 2015.

Antoniewicz, K. and Jasiński, M. (2016b). Nowe sterowanie predykcyjne 3-poziomowym 4-gałęziowym równoległym filtrem aktywnym – zastosowanie modelu o ograniczonej liczbie stanów. *Przeglad Elektrotechniczny*, 92(4), pp. 74–78.

Antoniewicz, K. and Rafal, K. (2017). Model Predictive Current Control Method for Four-Leg Three-Level Converter Operating as Shunt Active Power Filter and Grid Connected Inverter. *Bulletin of the Polish Academy of Sciences Technical Sciences*, 65(5), pp. 601–607.

Defay, F., Llor, A.-M. and Fadel, M. (2008). A Predictive Control With Flying Capacitor Balancing of a Multicell Active Power Filter. *IEEE Transactions on Industrial Electronics*, 55(9), pp. 3212–3220.

Falkowski, P. and Sikorski, A. (2018). Finite Control Set Model Predictive Control for Grid-Connected AC–DC Converters With LCL Filter. *IEEE Transactions on Industrial Electronics*, 65(4), pp. 2844–2852.

Grodzki, R., Sikorski, A. and Jasiński, M. (2011). Predykcyjne algorytmy sterowania trójfazowym przekształtnikiem AC/DC. *Przegląd Elektrotechniczny*, 87(6), pp. 105–110.

Orlowska-Kowalska, T., Blaabjerg, F. and Rodriguez, J. (2014). Advanced and intelligent control in power electronics and drives. In: J. Kacprzyk, ed., *Studies in Computational Intelligence.* Switzerland: Springer, pp. 181–265.

Rodriguez, J., Kazmierkowski, M. P., Espinoza, J. R., Zanchetta, P., Abu-Rub, H., Young, H. A. and Rojas, C. A. (2013). State of the Art of Finite Control Set Model Predictive Control in Power Electronics. *IEEE Transactions on Industrial Informatics*, 9(2), pp. 1003–1016.

Sobanski, P. (2017). Modified Scheme of Predictive Torque Control for Three-Phase Four-Switch Inverter-Fed Motor Drive With Adaptive DC-Link Voltage Imbalance Suppression. *Power Electronics and Drives*, 2(37), pp. 93–101.

Strzelecki, R. M. and Supronowicz, H. (2000). *Współczynnik mocy w systemach zasilania prądu przemiennego i metody jego poprawy*. Warsaw: Oficyna Wydawnicza Politechniki Warszawskiej. pp. 11–69.